Article:
Kwak, C.K., Perez, G.E., Freestone, B.G. et al. (4 more authors) (2016) Improved efficiency in organic solar cells via conjugated polyelectrolyte additive in the hole transporting layer. Journal of Materials Chemistry C . ISSN 2050-7526

https://doi.org/10.1039/C6TC03771B

Improved efficiency in organic solar cells via conjugated polyelectrolyte additive in the hole transporting layer

Chan Kyu Kwak[1], Gabriel E. Pérez[1], Benjamin G. Freestone[2], Sulaiman A. Al-Isaee[3], Ahmed Iraqi[3], David G. Lidzey[2], and Alan D. F. Dunbar[1*]

1 Department of Chemical and Biological Engineering, University of Sheffield, Sheffield, S1 3JD, UK
2 Department of Physics and Astronomy, University of Sheffield, Sheffield, S3 7RH, UK
3 Department of Chemistry, University of Sheffield, Sheffield, S3 7HF, UK
* Corresponding Author: a.dunbar@sheffield.ac.uk

Abstract

An anionic conjugated polyelectrolyte poly[(9,9-bis(4-sulfonatobutyl sodium) fluorene-alt-phenylene)-ran-(4,7-di-2-thienyl-2,1,3-benzothiadiazole-alt-phenylene)] which exhibits good solubility in water was synthesised via Suzuki-cross coupling. This conjugated polyelectrolyte was used as an additive in the hole transporting layer within organic photovoltaic devices. There is an efficiency gain as a result of an improved carrier generation and charge transport across the interface into the hole transport layer when the work function of the hole transport later is well matched to the active layer of the solar cell. The best performances were achieved using 5 mg/ml of the polyelectrolyte additive added to the hole transport layer solution in which case the average power conversion efficiency increased from 4.63 % for reference devices without any additive to 5.26 % when the additive is present which is a 13 % improvement. The reproducibility of device performance was also significantly improved with the variation in fill factor, short circuit current and open circuit voltage all improving when the additive is present.

Introduction

Organic solar cells (OSCs) are an attractive technology and a potential source of renewable and clean energy due to their low cost, light weight, mechanical flexibility, and use of green materials. [1] Recently, the power conversion efficiency (PCE) of OSCs has been improved up to 11.5 % due to developments in materials and fabrication processes. The most typical architecture for devices is a bulk heterojunction (BHJ) based on a polymer:fullerene blend for the active layer. Indium tin oxide (ITO) is used for the anode, Poly(3,4-ethylenedioxythiophene):Poly(styrenesulfonate) (PEDOT:PSS) for hole transporting layer (HTL), and aluminium for the cathode. [2]
Conjugated polyelectrolytes (CPEs) are conjugated polymers that contain charged ionic side chains which give them water-solubility. [3] CPEs are promising materials for chemical [4] and biological [5] sensors, thin film transistors, [6] organic light emitting diodes, [7] and organic solar cells. [8] During the past decade, CPEs have been used as electron transporting layers (ETLs) or HTLs in OSCs and CPE interlayers have helped to improve the PCE of devices. [8a, 8c, 9] He et al. and Zhou et al. reported fluorene and cyclopenta-dithiophene based CPEs as thin ETLs and HTLs, respectively and showed improvement in J_{SC}, V_{OC}, FF and PCE. He et al. reported that PTB7 based solar cells achieved PCEs over 8 % with a positively charged poly[(9,9-bis(3'-(N,N-dimethylamino)propyl)-2,7-fluorene)-alt-

2,7-(9,9–dioctylfluorene)] (PFN) interlayer; the device architecture was ITO/PEDOT:PSS/PTB7:$PC_{71}BM$/PFN/Ca/Al. [9c] Zhou et al. showed an improvement of J_{SC}, V_{OC}, FF and PCE using CPE-K negatively charged conjugated polyelectrolyte as a HTL instead of PEDOT:PSS. The solar cell performance was increased giving a PCE of 8.2 % using a device structure of ITO/CPE-K/PTB7:$PC_{71}BM$/Ca/Al. [9a]

Herein, we describe the use of a CPE additive in the PEDOT:PSS HTL to effectively increase the PCE and reproducibility of OSC performance. We synthesised poly[(9,9-bis(4-sulfonatobutyl sodium) fluorene-alt-phenylene)-ran-(4,7-di-2-thienyl-2,1,3-benzothiadiazole-alt-phenylene)] (PSFP-DTBTP) using fluorene, phenylene and di-thienyl-benzothiadiazole based conjugated polyelectrolyte. Fluorene, phenylene and thienyl units were introduced as electron donating groups and the benzothiadiazole units as the electron accepting groups in the conjugated polyelectrolyte. Sulfonate groups are attached to the fluorene backbone of the CPE to aid water solubility. The molar ratio of fluorene and di-thienyl-benzothiadiazole was 9:1. For this study, solar cells with a BHJ active layer consisting of blends of poly[N-9”-hepta-decanyl-2,7-carbazole-alt-5,5-(4’,7’-di-2-thienyl-2’,1’,3’-benzothiadiazole)] (PCDTBT) and [6,6]-phenyl-C71-butyric acid methyl ester ($PC_{71}BM$) and poly(3-hexylthiophene-2,5-diyl) (P3HT) with [6,6]-phenyl-C61-butyric acid methyl ester (PCBM) were fabricated. ITO and calcium/aluminium (Ca/Al) were used as the anode and cathode materials, respectively. Our OSC device architecture was ITO/PEDOT:PSS:PSFP-DTBTP/Active layer/(Ca)/Al and were compared to more standard ITO/PEDOT:PSS/Active layer/(Ca)/Al reference devices.

Experimental Section

Materials

All Materials for the synthesis of monomers and the polymer were purchased from Sigma-Aldrich, Acros Organics, Alfa Aesar, and Fisher scientific and used without further purification. PEDOT:PSS (Al 4083), PCDTBT, $PC_{71}BM$, ITO glass substrates, and UV-epoxy resin were purchased from Ossila Ltd.

Measurements

^{1}H and ^{13}C nuclear magnetic resonance (NMR) spectra were recorded by Bruker DRX-500 500 MHz NMR spectrometer in deuterium oxide (D_2O) or chloroform-d ($CDCl_3$). Elemental analysis (EA) results were measured using a Perkin Elmer 2400 series II. UV-vis absorption spectra were measured by an Ocean Optics USB2000+ spectrometer and DT-MINI-2-GS combined Deuterium-Halogen light source. Fourier transform infrared (FT-IR) spectra were recorded by Perkin Elmer Frontier MID FT-IR Spectrometer. Cyclic voltammetry (CV) measurements were obtained by Princeton Applied Research model 263A Potentiostat/Galvanostat. 10 ml of tetrabutylammonium perchlorate (0.1 M in acetonitrile) was used as the electrolyte solution. Ag/Ag^{+} reference electrode (Ag wire in 0.01 M $AgNO_3$ solution in the electrolyte solution), Pt working electrode (2mm diameter smooth Pt disc, area = 3.14×10^{-2} cm^2) and Pt counter electrode (Pt wire) were used as three electrode system for the measurement. Thickness of HTL thin films were measured by J. A. Woollam Co. M-2000 ellipsometer. The atomic force microscope (AFM) images were obtained by a Veeco Dimension 3100 AFM with a Nanoscope IIIa controller and basic extender. It was operated in tapping mode with Bruker TESPA tapping mode cantilevers with a nominal spring constant of 42 N/m and a nominal resonant frequency of 320 kHz. Photoluminescence spectra were collected by Keithley 2700 multimeter with Laser- LDCU CW 450nm diode laser and detector was silicon diode. Samples were measured under vacuum at approximately 1×10^{-3} mbar.

Synthesis of 2,7-dibromo-9,9-bis(4-sulfonatobutyl)fluorene disodium (1)[10]

100 mg of tetrabutylammonium bromide was dissolved in 50 wt % sodium hydroxide solution (10 ml) and DMSO (70 ml) under nitrogen and then 5 g (15.43 mmol) of 2,7-dibromofluorene was added into the mixture in a 250 ml three-necked round-bottomed flask. A solution of 1,4-butane sultone (5.25g, 38.58 mmol) and DMSO (26 ml) was added dropwise into the mixture under nitrogen. The mixture was stirred for 3 h at room temperature then the reaction mixture was precipitated into 500 ml of acetone. The crude product was isolated by filtration and washed with ethanol. The product was re-crystallised twice in acetone/H_2O then dried under vacuum at 40 °C for 24 h. The product was obtained as a white powder. Yield 6.28 g (63.56 %). ^{1}H NMR (500 MHz, D_2O, δ ppm): 7.62 (d, 2H), 7.59 (d, 2H), 7.47 (dd, 2H), 2.58-2.42 (m, 4H), 2.05-1.88 (m, 4H), 1.47-1.26 (m, 4H), 0.6-0.41 (m, 4H). ^{13}C NMR (125 MHz, D_2O, δ ppm): 167.75, 152.15, 138.88, 130.31, 126.47, 121.44, 121.26, 55.18, 50.76, 38.57, 24.24, 22.39. Element. Anal. Calcd. for $C_{21}H_{22}Br_2Na_2O_6S_2$: C, 39.39; H, 3.46; Br, 24.96; S, 10.01; found: C, 34.93; H, 3.67; Br, 21.18; S, 8.71.

Synthesis of 4,7-dibromo-2,1,3-benzothiadiazole (2)[11]

2,1,3-Benzothiadiazole (10 g, 73.4 mmol) and hydrobromic acid (150 ml, 48%) were added into a two-necked 500 ml round-bottomed flask and stirred. A mixture of bromine (35.19 g, 220.2 mmol) and hydrobromic acid (100 ml, 48%) was very slowly added dropwise into the flask. The mixture was heated under reflux for 6 h. Dark orange coloured solids were produced. The mixture was cooled down and neutralised with sodium bisulfite solution (~40 %, 250 ml) to remove excess bromine. The solids were filtered and washed well in water over 1h then washed with diethyl ether. The product was re-crystllized from chloroform/methanol and dried in vacuum at 40 °C for 24 h to affordyellowish crystals. Yield 15.9 g (73.7 %). ^{1}H NMR (500 MHz, $CDCl_3$, δ ppm): 7.75 (s, 2H). ^{13}C NMR (125 MHz, $CDCl_3$, δ ppm) 152.99, 132.38, 113.94. Element Anal. Calcd. for $C_6H_2Br_2N_2S$: C, 24.52; H, 0.69; Br, 54.36; N, 9.53; S, 10.91; found: C, 24.55; H, 0.73; Br, 53.36; N, 9.4; S, 10.22.

Synthesis of 4,7-di-2-thienyl-2,1,3-benzothiadiazole (3)[12]

A mixture of 4,7-dibromo-2,1,3-benzothiadiazole (1 g, 3.4 mmol) and thiophene-2-boronic acid pinacol ester (1.79 g, 8.5 mmol) was dissolved in anhydrous toluene (30 ml). Na_2CO_3 2M aqueous (10 ml) was then added under nitrogen followed by $Pd(OAc)_2$/tri(o-tolyl)phosphine (1/2, 4 mol %) and then the mixture was stirred at 95 °C under reflux for 24 h. After cooling the mixture, water was added to the flask. The organic phase was separated and then washed with water and brine. The organic phase was dried over $MgSO_4$ and then evaporated. The product was purified by column chromatography using dichloromethane (DCM)/hexane (1/3, v/v). The solid was recrystallized in toluene/ethanol. The product was dried in vacuum at 40 °C for 24 h. Red crystals were obtained. Yield 0.33 g (32.3 %). ^{1}H NMR (500 MHz, $CDCl_3$, δ ppm): 8.11 (dd, 2H), 7.88 (s, 2H), 7.45 (dd, 2H), 7.21 (dd, 2H). ^{13}C NMR (125 MHz, $CDCl_3$, δ ppm): 152.5, 139.3, 128.1, 127.5, 126.8, 126, 125.8. Element Anal. Calcd. for $C_{14}H_8N_2S_3$: C, 55.97; H, 2.68; N, 9.33; S, 32.02; found: C, 56.15; H, 3.06; N, 9.07; S, 30.85.

Synthesis of 4,7-bis(5-bromo-2-thienyl)-2,1,3-benzothiadiazole(4)[11, 13]

4,7-Di-2-thienyl-2,1,3-benzothiadiazole (0.3 g, 1 mmol) was dissolved in a mixture of chloroform (7 ml) and acetic acid (7 ml) in a flask. N-bromosuccinimide (NBS) (0.4 g, 2.2 mmol) was then slowly

added into the mixture. The mixture was stirred at room temperature overnight (about 20 hours). Dark red solids precipitated out of solution and were filtered off. The product was washed with methanol and then recrystallized in DMF. Dark red crystals were obtained. Yield 0.29 g (63.8 %). ^{1}H NMR (500 MHz, $CDCl_3$, δ ppm): 7.80 (dd, 2H), 7.78 (s, 2H), 7.15 (dd, 2H). Element Anal. Calcd. for $C_{14}H_6Br_2N_2S_3$: C, 36.70; H, 1.32; Br, 34.88; N, 6.11; S, 20.99; found: C, 29.93; H, 1.08; Br, 48.66; N, 4.92; S, 17.10.

Synthesis of poly[(9,9-bis(4-sulfonatobutyl sodium) fluorene-alt-phenylene)-ran-(4,7-di-2-thienyl-2,1,3-benzothiadiazole-alt-phenylene)] (PSFP-DTBTP) [5b]

2,7-Dibromo-9,9-bis(4-sulfonatobutyl)fluorene disodium (0.63 g, 0.98 mmol), 4,7-bis(5-bromo-2-thienyl)-2,1,3-benzothiadiazole (0.05 g, 0.11 mmol), and 1,4-phenylene-bisboronic acid pinacol ester (0.36 g, 1.09 mmol) were dissolved in a mixture of DMF (10 ml) and Na_2CO_3 2M aqueous (15 ml) in a 100 ml round-bottomed flask. After the materials completely dissolved, $Pd(OAc)_2$/tri(o-tolyl)phosphine (1/4, 5 mol %) was added and the mixture was then degassed. The reaction mixture was stirred at 85-90 °C under reflux for 3 days. The mixture was cooled to room temperature and poured into acetone. The precipitate was redissolved in deionised water. The solution was dialyzed in cellulose membrane (MWCO 12,400) for 3 d. The reddish product was obtained through freeze-drying, yield 0.22 g (37%).^{1}H NMR (500 MHz, D_2O, δ ppm): 8.39-6.78 (br, 10H), 3.88-3.51 (br, 3.6H), 2.68-2.02 (br, 3.6H), 1.58-1.09 (br, 3.6H), 0.83-0.6 (br, 3.6H).

Result and Discussion

Synthesis of conjugated polyelectrolyte

The chemical structures and synthesis procedure of PSFP-DTBTP are illustrated in Scheme 1. 2,7-Dibromo-9,9-bis(4-sulfonatobutyl)fluorene disodium (1) was prepared on reacting 2,7-dibromofluorene in a mixture of dimethyl sulfoxide (DMSO) and 50 wt % sodium hydroxide (NaOH) solution with 1,4-butane sultone in the presence of tetrabutylammonium bromide (TBAB). 4,7-Dibromo-2,1,3-benzothiadiazole (2) was prepared via the bromination of benzothiadiazole with bromine in hydrobromic acid (HBr). 4,7-Di-2-thienyl-2,1,3-benzothiadiazole (3) was synthesised via the Suzuki cross-coupling of (2) and thiophene-2-boronic acid pinacol ester using $Pd(OAc)_2$/tri(o-tolyl)phosphine as catalyst in toluene and 2M aqueous Na_2CO_3 as a base. 4,7-Bis(5-bromo-2-thienyl)-2,1,3-benzothiadizole (4) was prepared through the bromination of (3) using N-bromosuccinimide (NBS) in a mixture of chloroform and acetic acid. PSFP-DTBTP was synthesised through the Suzuki cross-coupling polymerisation of (1), (4), and 1,4-phenylene-bisboronic acid pinacol ester at a molar ratio of 9:1:10 in N,N-dimethylformamide (DMF) using 2M aqueous Na_2CO_3 as a base in the presence of $Pd(OAc)_2$/tri(o-tolyl)phosphine as a catalyst. The PSFP-DTBTP was purified by dialysis using a dialysis membrane (molecular weight cut-off: 12.4 KDa) for 3 days to get the final product with 37% yield. In order to synthesise a low band gap based CPE, a fluorene, phenylene and thienyl units were used as electron donating groups and benzothiadiazole units were used as electron accepting groups. The sulfonatobutyl side chains on the fluorene repeat units in a molar ratio of 9:1 of (1) and (4) afford good solubility of the resulting CPE in water.

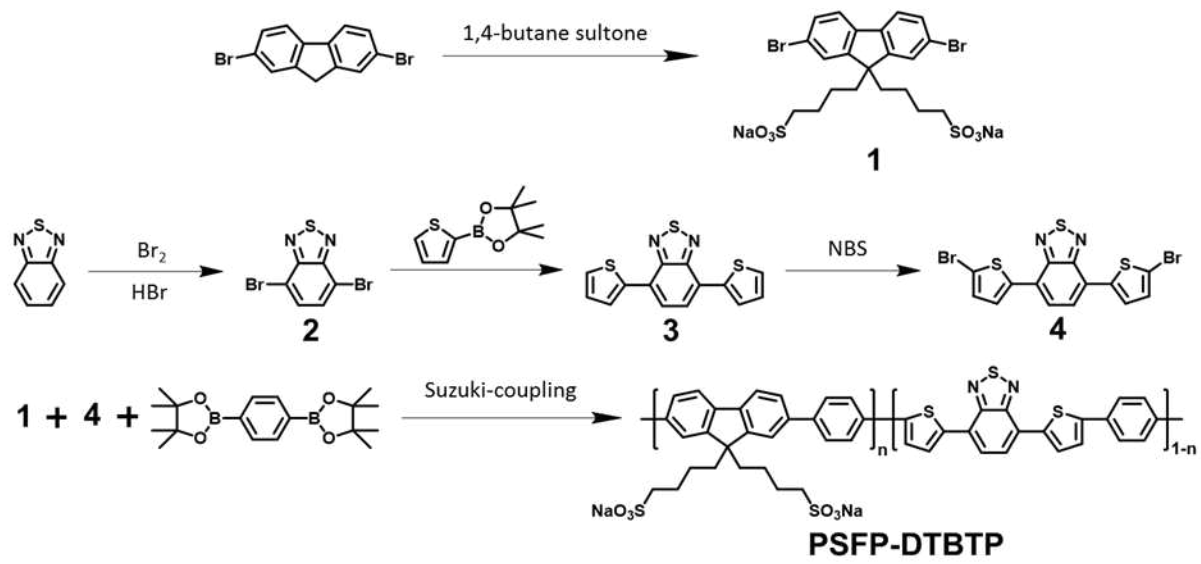

Scheme 1 Procedure of polymer synthesis.

Optical characterisation of conjugated polyelectrolyte

Hole transporting layer blends of PEDOT:PSS:PSFP-DTBTP were prepared by adding 2 mg/ml or 5 mg/ml or 8 mg/ml of the CPE to the PEDOT:PSS Al 4083 solution (1.3 – 1.7 wt%, Ossila Ltd) and were named as HTL2, HTL5, and HTL8 respectively in this paper. To measure the UV-vis absorption of thin films, PSFP-DTBTP, PEDOT:PSS, HTL2, HTL5, and HTL8 were spin coated at 6000 rpm on glass substrates for 40 s and then thermally annealed at 150 °C for 15 min. Figure 1 (a) shows the UV-vis absorption spectra of PSFP-DTBTP solution in water and thin films of PSFP-DTBTP, PEDOT:PSS, HTL2, HTL5, and HTL8 after spin casting onto glass substrates. The inset photo of Figure 1 (a) is PSFP-DTBTP (5mg/ml) in deionised water showing its red colour. The PSFP-DTBTP film shows a strong $\pi-\pi^*$ absorption peak at 366 nm from fluorene, phenylene and thienyl groups and a very weak absorption peak at around 530 nm from intramolecular charge transfer between donor and acceptor units along polymer chains. The 366 nm absorption peak observed in the PSFP-DTBTP film was shifted by about 8 nm compared to the solution spectra where the peak was at about 358 nm. The number of co-planar rings along the backbone of the polymer determines its conjugation length. The longer the conjugation length, the smaller the separation between adjacent energy levels due to quantum confinement effects. Fewer twists in the polymer increases the co-planarity and can result from changes in the environment. Therefore the absorbance shift is attributed to increasing the conjugation length of the rigid backbone in the film, when the polymer is in the solid state. However, we could not confirm whether the peak from the DTBTP group around 530 nm was shifted in comparison to solution because of the weak signal strength. The pristine PEDOT:PSS film did not show any specific absorption features. The HTL films showed a small absorption peak at 372 nm which increased with increasing concentration (2 mg/ml, 5 mg/ml and 8 mg/ml) and it has very small trace of an absorption peak at around 530 nm from PSFP-DTBTP. The main absorption peaks of HTL2 and HTL5 were slightly red shifted from the PSFP-DTBTP peak at 366 nm to 372 nm. However, HTL8 was blue shifted and had an absorption peak at 362 nm.

Although PSFP-DTBTP has a very weak peak at around 530 nm, the spectral edge of the polymer absorption is around 600 nm which equates to a band gap for PSFP-DTBTP of 2.0 eV from the UV-vis absorption spectra data which is in good agreement with the cyclic voltammetry (CV) measurement in Figure 2.

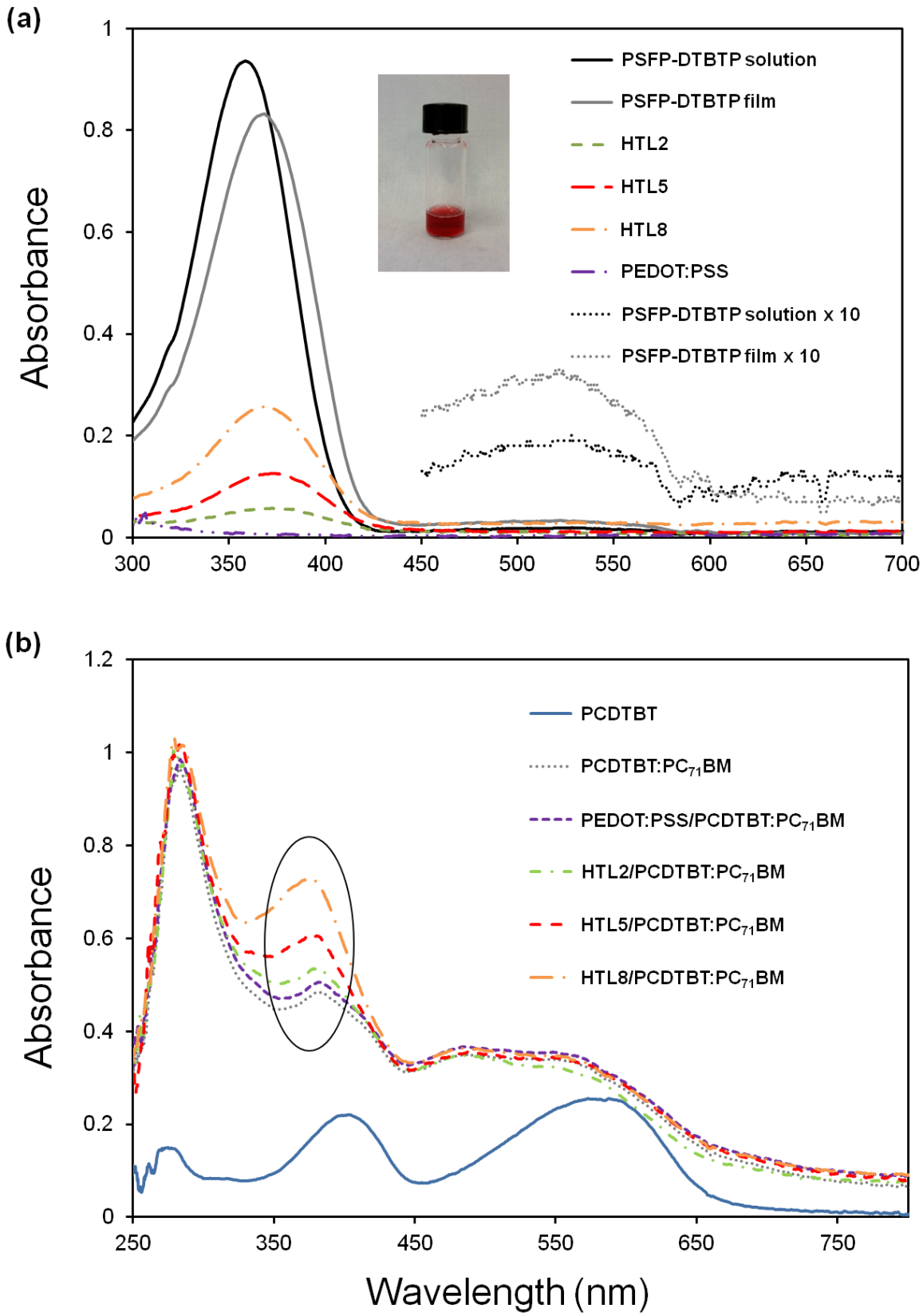

Figure 1 UV-vis absorption spectra of (a)PSFP-DTBTP solution (black solid) and films of PSFP-DTBTP (grey solid), HTL2 (green), HTL5 (red), HTL8 (orange), PEDOT:PSS (purple), increased x 10 peaks of PSFP-DTBTP solution (black dot) and PSFP-DTBTP film (grey dot), (inset photo is PSFP-DTBTP solution), and (b) PCDTBT (blue), PCDTBT:$PC_{71}BM$ (grey), PEDOT:PSS/PCDTBT:$PC_{71}BM$ (purple), and HTL2 (green), or HTL5 (red), HTL8/PCDTBT:$PC_{71}BM$ (orange) (HTL is hole transporting layer of PEDOT:PSS:PSFP-DTBTP).

In order to understand the combined absorption abilities of the active layer and HTLs, Figure 1 (b) shows the UV-vis absorption spectra of PCDTBT, PCDTBT:$PC_{71}BM$ (blend ratio of 1:4) and HTL/PCDTBT:$PC_{71}BM$. All HTLs were spin coated on glass substrates at 6000 rpm and the HTLs were thermally annealed at 150 °C for 15 min then PCDTBT:$PC_{71}BM$ were spin coated at 700 rpm on the HTL and thermally annealed at 80 °C for 15 min. The PCDTBT film showed a strong absorption peak at 403 nm and strong broad absorption band from 560 nm to 590 nm. [14] The blend of PCDTBT:$PC_{71}BM$ film showed increased absorption ability from 300 nm to 580 nm due to absorption by $PC_{71}BM$. PEDOT:PSS/PCDTBT:$PC_{71}BM$ did not show any specific difference with PCDTBT:$PC_{71}BM$. However, HTL2, HTL5, and HTL8/PCDTBT:$PC_{71}BM$ films showed an increasing peak around 370 nm with increasing CPE concentration in the HTL and this corresponds with the results for the PSFP-DTBTP absorption peak in Figure 1 (a).

A CV measurement was used to study the oxidation and reduction properties of the polyelectrolyte. The CV measurement of the conjugated polyelectrolyte was performed in the presence of tetrabutylammonium perchlorate (0.1 M) as an electrolyte in acetonitrile and Ag/Ag^+ reference electrode (Ag wire in 0.01 M $AgNO_3$ solution). A CV curve of PSFP-DTBTP is shown in Figure 2. The onset point of oxidation is 0.66 V and the energy level of the highest occupied molecular orbital (HOMO) was calculated at -5.37 eV. The reduction onset point is -1.33 V and the energy level of lowest unoccupied molecular orbital (LUMO) was calculated at -3.38 eV. These results were compared to a similar CPE material PFN (fluorene groups are included). The energy levels compared well with PFN (HOMO of -5.61 eV, and LUMO of -2.14 eV). [9b] The effect of the fluorene side group and the donor and acceptor nature of PSFP-DTBTP resulted in a lower oxidation and reduction potential than PFN. The ionic sulfonyl groups of PSFP-DTBTP lead to easier oxidation than general fluorene and DTBTP groups gave the polymer a lower reduction potential and lower band gap than PFN due to the alternating donor-acceptor structure of the polymer. [8d]

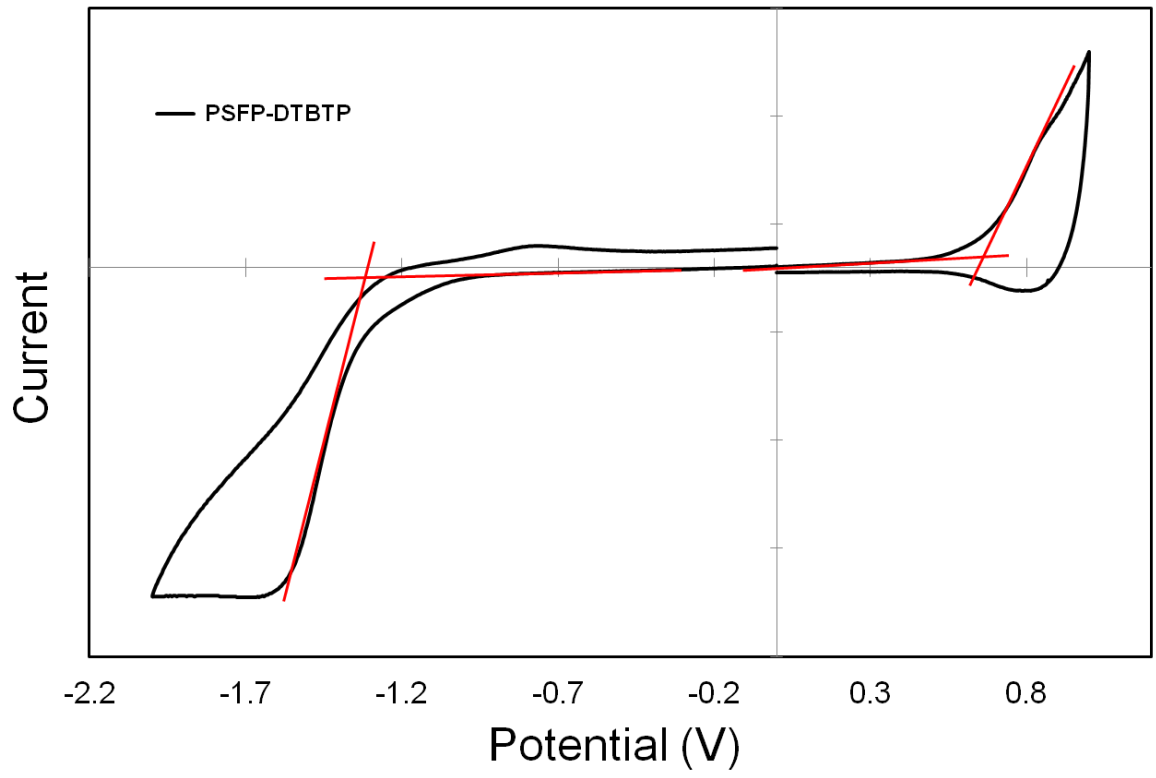

Figure 2 Cyclic Voltammetry (CV) diagram of PSFP-DTBTP.

Figure 3 (a) summarises the energy levels of ITO, PEDOT:PSS, PSFP-DTBTP, P3HT, PCDTBT, $PC_{71}BM$, PCBM, Ca, and Al and these are similar to those reported elsewhere. [2b, 15] As shown in Figure 3 (a), the HOMO level of PSFP-DTBTP is located between the HOMO level of PCDTBT and PEDOT:PSS, so holes generated in PCDTBT would easily move to the ITO electrode. Also electrons are blocked from going to ITO anode. In addition, extra absorption by the PSFP-DTBTP means it is possible to create electrons and holes in the PSFP-DTBTP. Therefore, some additional electrons may be injected into the PCDTBT and $PC_{71}BM$ and on to the cathode whilst and the additional holes move to the ITO anode via the PEDOT:PSS. However, in comparison the HOMO and LUMO levels of PSFP-DTBTP are lower than HOMO and LUMO levels of P3HT, respectively, so in the P3HT devices the PSFP-DTBTP would disrupt the flow of holes to the anode because it will act as a potential barrier. As a result, the P3HT devices with PSFP-DTBTP showed a reduction of PCE as described in Figure 4 (c) and Table 1.

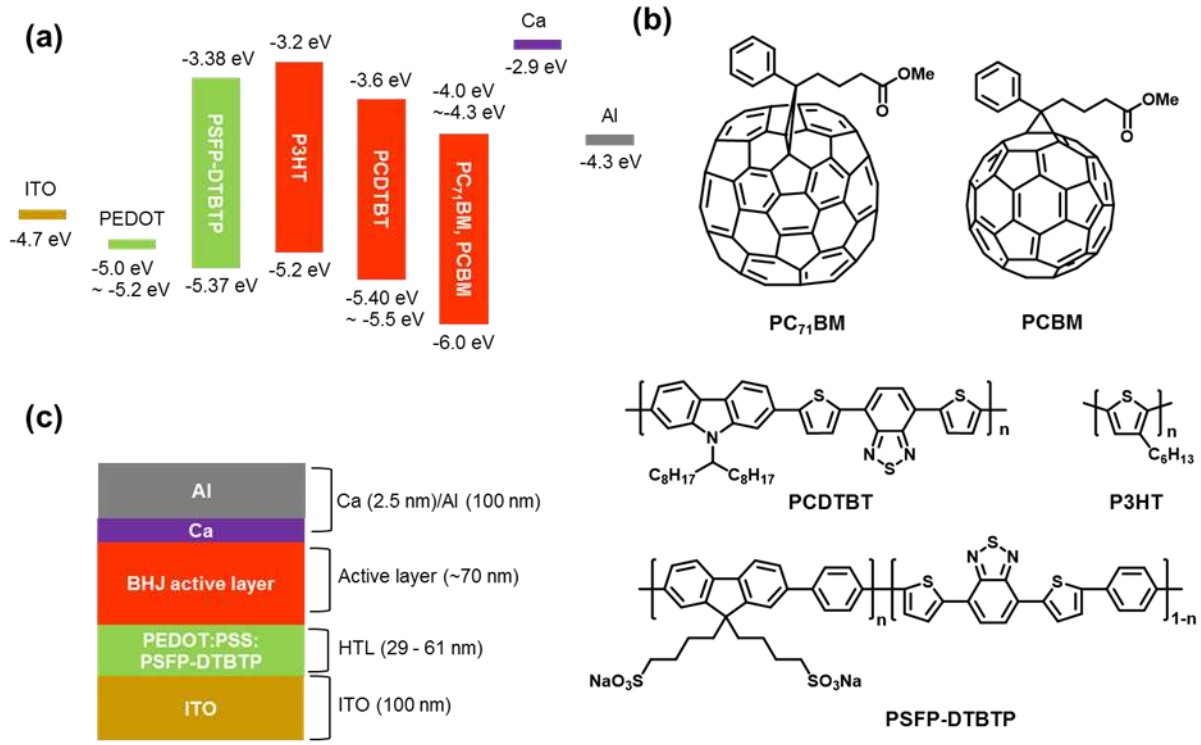

Figure 3 (a) The energy diagram of materials in a solar cell (PSFP-DTBTP band gap is measured by CV, others are from previous reports [2b, 15]), (b) the structure of PSFP-DTBTP, PCDTBT, and $PC_{71}BM$, and (c) the architecture of BHJ organic solar cell.

Work function of HTLs

The work functions of pristine PEDOT:PSS, and PSFP-DTBTP mixed PEDOT:PSS thin films were measured by ultraviolet photoelectron spectroscopy (UPS) using a helium lamp at 21.2 eV. The UPS spectra of PEDOT:PSS, HTL2, HTL5 and HTL8 are shown in Figure 4. The work function is seen as a "cut-off" in the UPS spectrum at the low kinetic energy side. As shown in Figure 4, the work function of PEDOT:PSS. HTL2, HTL5, and HTL8 are 4.95, 5.07, 5.14, and 5.11 eV, respectively. The HTL5 has a lower work function than the others and so is expected to show a higher V_{OC} than the devices made with the other HTL concentrations.

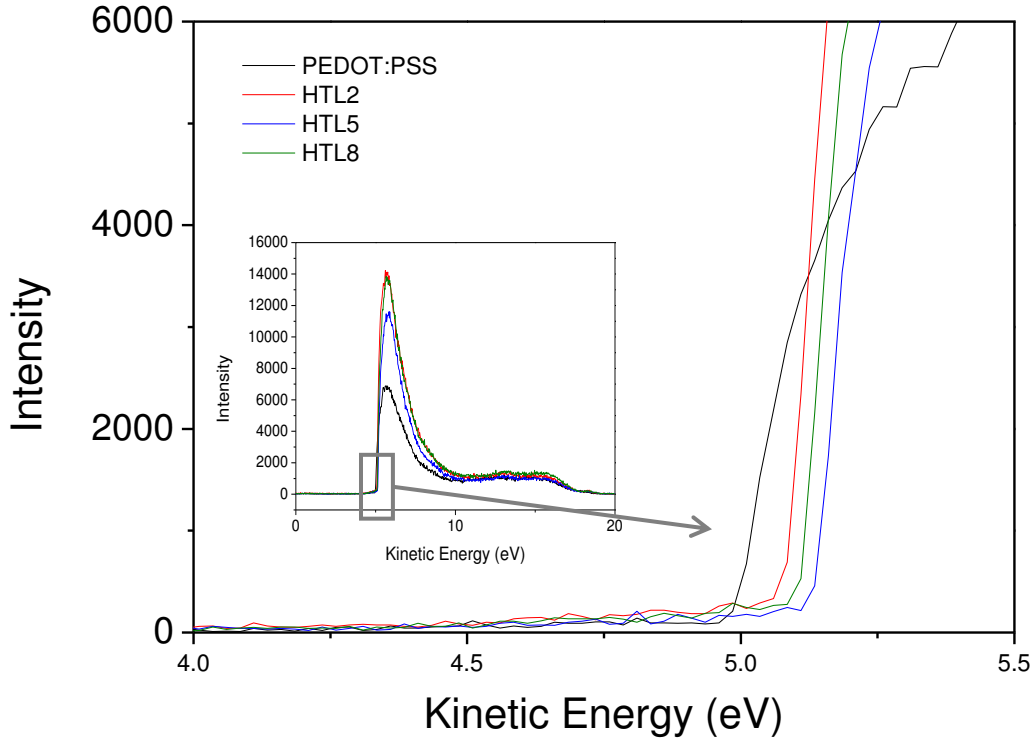

Figure 4 The UPS spectra of PEDOT:PSS, HTL2, HTL5, and HTL8 thin films

Photovoltaic properties

The architecture of the PCDTBT solar cells consisted of ITO/PEDOT:PSS, or HTL2, or HTL5, or HTL8/PCDTBT:$PC_{71}BM$/Ca/Al and the P3HT solar cells were ITO/PEDOT:PSS, or HTL5/P3HT:PCBM/Al. The device's structure, materials, and energy level of each material are described in Figure 3 (c). The corresponding J-V curves and external quantum efficiency (EQE) of the devices are shown in Figure 5 and their photovoltaic characteristics are described in Table 1. The J-V curves of the solar cell devices were measured using a solar simulator under AM 1.5G irradiation. Reference PCDTBT devices showed a J_{SC} of -8.63 ± 1.7 mA/cm^2, V_{OC} of 0.84 ± 0.03 V, and FF of 62.28 ± 7.85 %. The average PCE was 4.63 % and the best PCE was 5.36 %. HTL2 devices and HTL8 devices showed better efficiency on average, but the reference devices recorded a better champion PCE than HTL2 and HTL8. However, HTL5 devices recorded a J_{SC} of -9.46 ± 0.88 mA/cm^2, V_{OC} of 0.88 ± 0.03 V, FF of 66.25 ± 2.85 %, with an average PCE of 5.26 % and a best PCE of 5.67 %, which are significantly better results than all the other devices. In general, enhancement of all parameters J_{SC}, V_{OC}, and FF in HTL5 device resulted in an improvement of both average and best efficiency. The devices with CPE added showed a higher V_{OC} by about 0.02 – 0.04 V compared to the reference device. The ideal maximum V_{OC} in solar cells is determined by the difference between the HOMO level of the donor and the LUMO level of the acceptor, but the V_{OC} in actual devices showed a value lower than this ideal V_{OC}. The actual V_{OC} is affected by the work function of electrodes and any interfacial layer. [16] The devices with CPE added have a lower work function (-5.14 eV) than the pristine PEDOT:PSS (-4.95 eV) which gave the devices with CPE added a higher V_{OC} than the reference devices. In Figure 5 (b), the HTL5 device showed a lower EQE than the pristine PEDOT:PSS device below 390 nm. This is attributed to some of the light 330 nm to 420 nm being

absorbed by the CPE rather than PCDTBT and therefore not undergoing efficient charge separation across the interfaces within the BHJ. However, as demonstrated below in our PL experiments, significant energy transfer can occur between the CPE and PCDTBT which minimises this effect. Above 390 nm the EQE of the HTL5 device is higher than that of the PEDOT:PSS device, which is attributed to improved charge transfer into the HTL because of the improved match between the work function of the HTL and the PCDTBT BHJ layer HOMO level. The HTL5 device has a higher J_{sc} than the pristine PEDOT:PSS based device because the charge transport is more efficient. Fewer generated charges are lost to recombination processes.

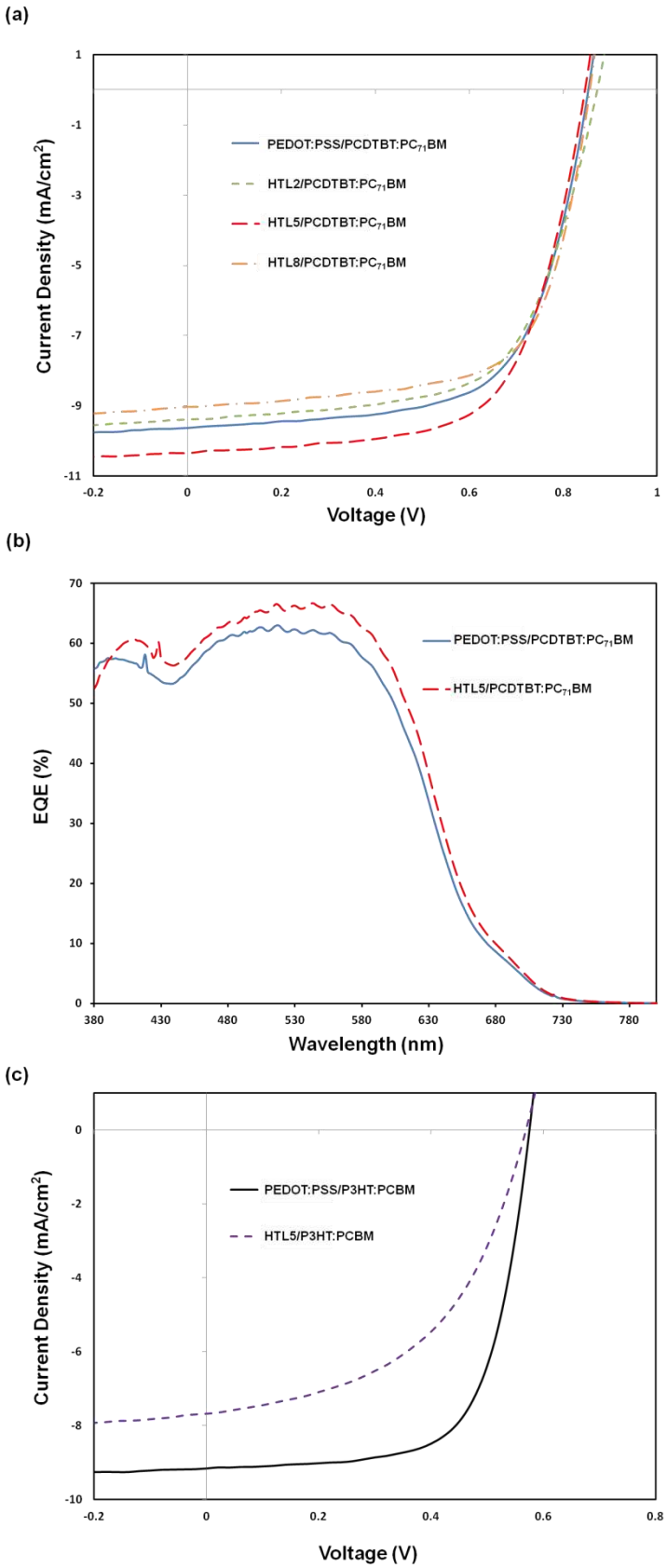

Figure 5 (a) J-V curves of PEDOT:PSS/PCDTBT:PC_{71}BM (blue), HTL2/PCDTBT:PC_{71}BM (green), HTL5/PCDTBT:PC_{71}BM (red), and HTL8/PCDTBT:PC_{71}BM (orange) solar cells. (b) EQE of the PEDOT:PSS/PCDTBT:PC_{71}BM (blue) and HTL5/PCDTBT:PC_{71}BM (red) solar cell. (c) J-V curves of PEDOT:PSS/P3HT:PCBM (black) and HTL5/P3HT:PCBM (purple) solar cells.

Table 1. Photovoltaic properties of PCDTBT and P3HT solar cells with various HTL (The average value was calculated with the best 50 % of pixels of over 6 devices.).

HTL	Device amounts	HTL Thickness	J_{SC} (mA/cm^2)	V_{OC} (V)	FF (%)	PCE (%)	
						Average	Best
PCDTBT solar cells							
PEDOT: PSS	15	29 nm	-8.63 ± 1.7	0.84 ± 0.03	62.28 ± 7.85	4.63	5.32
HTL2	7	35 nm	-8.88 ± 0.54	0.86 ± 0.04	62.51 ± 6.79	4.83	5.18
HTL5	15	47 nm	-9.46 ± 0.88	0.88 ± 0.03	66.25 ± 2.85	5.26	5.67
HTL8	7	61 nm	-8.84 ± 0.53	0.86 ± 0.03	63.62 ± 4.42	4.85	5.18
P3HT solar cells							
PEDOT: PSS	6	29 nm	-8.99 ± 0.18	0.56 ± 0.01	66.55 ± 0.81	3.35	3.55
HTL5	6	47 nm	-6.83 ± 0.98	0.57 ± 0.01	40.54 ± 9.46	1.68	2.18

Conductivity of the hole transporting layer

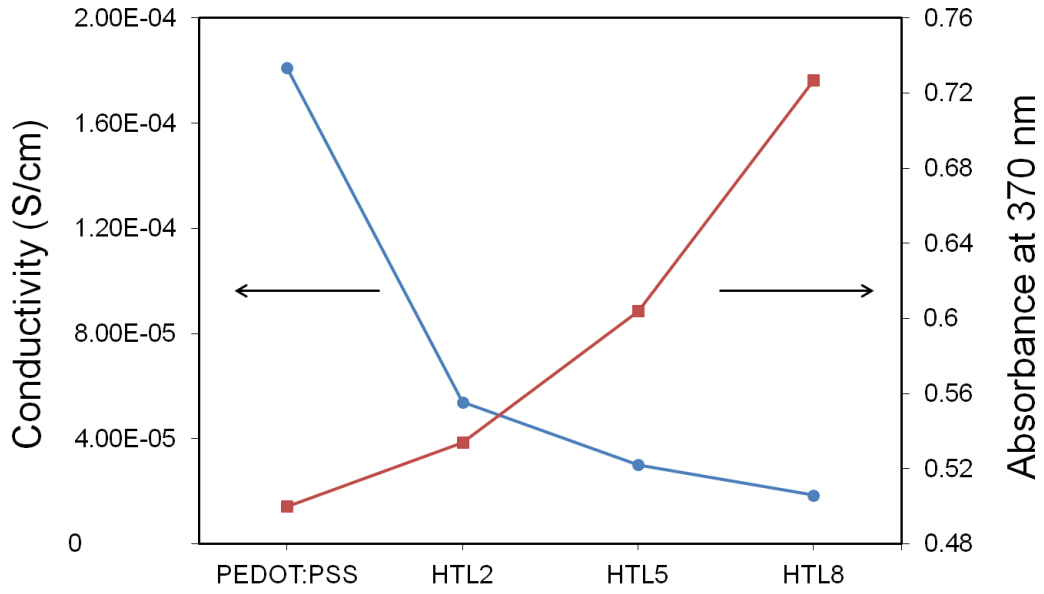

Figure 6 Effect of PSFP-DTBTP concentration on the film conductivity for the hole transporting layers (blue) and the film UV-vis absorption at 370 nm for the hole transporting layers.

The conductivity and absorption values of the HTL are described in Figure 6. In Figure 6, the pristine PEDOT:PSS shows the highest sheet conductivity 1.8 x 10^{-4} S/cm and HTL2, HTL5, and HTL8 show a decrease of conductivity 5.4 x 10^{-5} S/cm, 3.0 x 10^{-5} S/cm, and 1.8 x 10^{-5} S/cm respectively with increase of concentration of PSFP-DTBTP in the films. Therefore, assuming the carrier conductivity through the HTL film follows the same trend as the sheet conductivity the presence of CPE in the

HTL would be expected to reduce performance. The PSFP-DTBTP would act as an insulator in the HTL, but yet the HTL5 based solar cell showed the best efficiency. Considering the absorbance of these devices the incident light will be absorbed more efficiently between 330 nm and 420 nm in those devices with CPE in the HTL layers compared to the pristine PEDOT:PSS. The presence of CPE therefore increases absorbance and results in the generation of more excitons which may diffuse to the accepting group in the CPE to then be separated into free electrons and holes with the electrons transferring to the active layer and the holes to the PEDOT:PSS. Therefore, although the CPE mixed with PEDOT:PSS showed lower conductivity than that of PEDOT:PSS, the HTL5 based solar cell had a higher PCE than that of pristine PEDOT:PSS based solar cell because, PSFP-DTBTP transfers some electrons from the HTL to the BHJ layer. There is a trade-off between reduced conductivity through the HTL layer and improved carrier generation and charge transport across the interface into the HTL layer which is optimised at a CPE concentration close to 5 mg/ml.

To demonstrate that the energy level alignment between the HTL and the PCDTBT in the BHJ plays an important role in this efficiency enhancement P3HT solar cells were also fabricated with CPE added to the HTL. P3HT has a HOMO level which (unlike PCDTBT) is not well matched to the HTL with CPE additive. The reference P3HT solar cell showed a J_{SC} of -8.99 ± 0.18 mA/cm^2, V_{OC} of 0.56 ± 0.01 V, FF of 66.55 ± 0.81 %, average PCE of 3.35 % and the best PCE of 3.55 %. However, the HTL5 based P3HT solar cell showed lower performance characteristics with a J_{SC} of -6.83 ± 0.98 mA/cm^2, V_{OC} of 0.57 ± 0.01 V, FF of 40.54 ± 9.46 %, average PCE of 1.68 %, and the best PCE of 2.18 %. HTL5 based P3HT exhibited a similar V_{OC} (0.01 V increased) with reference P3HT due to lower HOMO level of HTL5. The J_{sc} was significantly reduced because the HOMO energy level of PSFP-DTBTP is lower than that of P3HT and therefore the energy transfer across this interface is reduced because there is an effective energy barrier to hole transport across this interface, reducing the efficiency of charge transport.

Photoluminescence characterisation of hole transporting layer and active layer

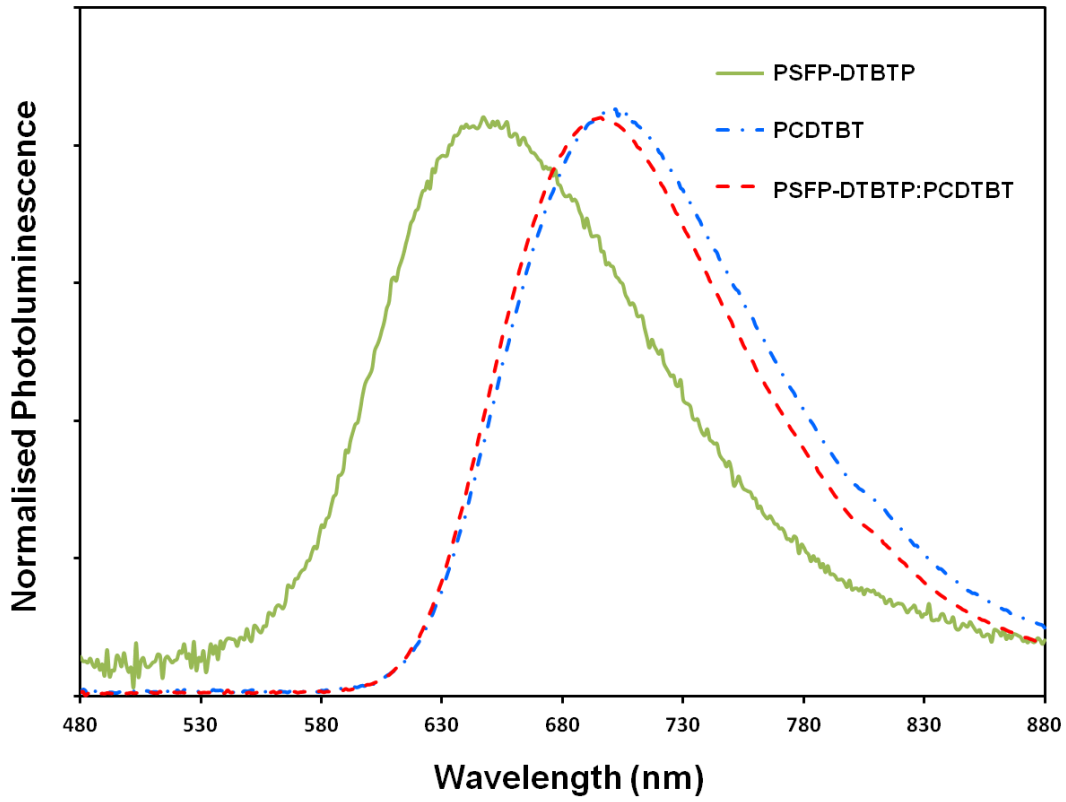

Figure 7 Normalized PL spectra of films of PSFP-DTBTP, PCDTBT and bi-layer of PSFP-DTBTP and PCDTBT.

Figure 7 showed the photoluminescence (PL) spectra of PSFP-DTBTP (15 mg/ml in H_2O) film, PCDTBT (4 mg/ml in chlorobenzene) film, and PSFP-DTBTP and PCDTBT bi-layer film. The PL spectrum of PCDTBT showed an emission peak at 698 nm and small shoulder peak at 810 nm. It is similar to the emission peak of PCDTBT from a previous report. [8a] PCDTBT was well quenched with $PC_{71}BM$ in a blend (1:4 weight ratio) film in Figure S2. The PL spectrum of PSFP-DTBTP film has an emission peak at 647 nm, shifted considerably from the strong absorption peak at 366 nm (Figure 1 (b)). This red emission is due to exciton migration from the electron donating fluorene group to the electron accepting benzothiadiazole group in the polyelectrolyte. [17] The PL spectra of PEDOT:PSS with PSFP-DTBTP are illustrated in Figure S3. PEDOT:PSS thin films with the CPE additive showed a very weak PL peak around 647 nm. To understand the correlation between the HTL5 and PCDTBT, a PSFP-DTBTP and PCDTBT bi-layer film was prepared. The PL spectra of the PSFP-DTBTP and PCDTBT bi-layer film did not exhibit an emission peak similar to the PSFP-DTBTP only film at 647 nm (Figure 7) but instead showed an emission peak at 695 nm. This is attributed to the overlapping of the PSFP-DTBTP emission peak with absorption peak of PCDTBT around 600 nm to 650 nm and the resulting quenching of the PSFP-DTBTP emission by PCDTBT. It implies that intermolecular charge transfer was occurring from the CPE to the PCDTBT. [18] Therefore, much of the light absorbed by the CPE in our devices will likely be transferred to the PCDTBT minimising losses.

Conclusion

A conjugated polyelectrolyte was synthesised from 9,9-bis(4-sulfonatobutyl sodium) fluorene, phenylene, and 4,7-di-2-thienyl-2,1,3-benzothiadiazole units using a Suzuki-cross coupling reaction. The conjugated polyelectrolyte synthesised dissolved well in water. Poly[(9,9-bis(4-sulfonatobutyl

sodium) fluorene-alt-phenylene)-ran-(4,7-di-2-thienyl-2,1,3-benzothiadiazole-alt-phenylene)] (PSFP-DTBTP) showed a strong absorption peak at 370 nm with small absorption features around 550 nm, and a PL emission peak at 645 nm. The conjugated polyelectrolyte was used as an additive in the hole transporting layer of OSCs. The PSFP-DTBTP HTL based solar cell had a PCE of 5.67 % when incorporated in a PCDTBT:$PC_{71}BM$ solar cell which was a significant improvement over the control device without any CPE. All characteristics of the solar cell with CPE were higher than that of the reference device without the additive. The consistency of the device fabrication process was also improved. Although the HTL with the conjugated polyelectrolyte had a lower conductivity, the improved absorption ability of polyelectrolyte and the improved charge transport from the HTL more than compensated for this. In addition, the work function of the HTL with CPE added was lower than the pristine PEDOT:PSS, this results in the HTL5 device showing a higher V_{OC} by about 0.02-0.04 V compared to the PEDOT:PSS reference device. The work function for HTL5 is also better matched to the HOMO level of the PCDTBT within the BHJ layer. For this reason the improved performance of this device is mainly attributed to improved hole charge transfer from active layer BHJ to the HTL. The solar cell with 5 mg/ml CPE showed an average PCE improvement of 13 % compared to the reference device.

Reference

1. (a) Sondergaard, R.; Hosel, M.; Angmo, D.; Larsen-Olsen, T. T.; Krebs, F. C., Roll-to-roll fabrication of polymer solar cells. *Mater Today* **2012,** *15* (1-2), 36-49; (b) Espinosa, N.; Hosel, M.; Angmo, D.; Krebs, F. C., Solar cells with one-day energy payback for the factories of the future. *Energ Environ Sci* **2012,** *5* (1), 5117-5132; (c) Azzopardi, B.; Emmott, C. J. M.; Urbina, A.; Krebs, F. C.; Mutale, J.; Nelson, J., Economic assessment of solar electricity production from organic-based photovoltaic modules in a domestic environment. *Energ Environ Sci* **2011,** *4* (10), 3741-3753; (d) Gunes, S.; Neugebauer, H.; Sariciftci, N. S., Conjugated polymer-based organic solar cells. *Chem Rev* **2007,** *107* (4), 1324-1338; (e) Yu, G.; Gao, J.; Hummelen, J. C.; Wudl, F.; Heeger, A. J., Polymer Photovoltaic Cells - Enhanced Efficiencies Via a Network of Internal Donor-Acceptor Heterojunctions. *Science* **1995,** *270* (5243), 1789-1791; (f) Dennler, G.; Scharber, M. C.; Brabec, C. J., Polymer-Fullerene Bulk-Heterojunction Solar Cells. *Adv Mater* **2009,** *21* (13), 1323-1338.

2. (a) NREL http://www.nrel.gov/ncpv/images/efficiency_chart.jpg; (b) Thompson, B. C.; Frechet, J. M. J., Organic photovoltaics - Polymer-fullerene composite solar cells. *Angew Chem Int Edit* **2008,** *47* (1), 58-77; (c) Iyer, S. S. K.; Bajaj, D.; Bhat, A., Photovoltaic behaviour of organic polymer - PCBM bulk hetero junctions solar cells. *Iete J Res* **2006,** *52* (5), 391-399; (d) Benanti, T. L.; Venkataraman, D., Organic solar cells: An overview focusing on active layer morphology. *Photosynth Res* **2006,** *87* (1), 73-81.

3. (a) Huang, F.; Wang, X. H.; Wang, D. L.; Yang, W.; Cao, Y., Synthesis and properties of a novel water-soluble anionic polyfluorenes for highly sensitive biosensors. *Polymer* **2005,** *46* (25), 12010-12015; (b) Tran-Van, F.; Carrier, M.; Chevrot, C., Sulfonated polythiophene and poly (3,4-ethylenedioxythiophene) derivatives with cations exchange properties. *Synthetic Met* **2004,** *142* (1-3), 251-258; (c) Huang, F.; Wu, H. B.; Wang, D.; Yang, W.; Cao, Y., Novel electroluminescent conjugated polyelectrolytes based on polyfluorene. *Chem Mater* **2004,** *16* (4), 708-716; (d) Stork, M.; Gaylord, B. S.; Heeger, A. J.; Bazan, G. C., Energy transfer in mixtures of water-soluble oligomers: Effect of charge, aggregation, and surfactant complexation. *Adv Mater* **2002,** *14* (5), 361-366; (e) Gaylord, B. S.; Wang, S. J.; Heeger, A. J.; Bazan, G. C., Water-soluble conjugated oligomers: Effect of chain length and aggregation on photoluminescence-quenching efficiencies. *J Am Chem Soc* **2001,** *123* (26), 6417-6418.

4. (a) Son, J. H.; Jang, G.; Lee, T. S., Synthesis of water-soluble, fluorescent, conjugated polybenzodiazaborole for detection of cyanide anion in water. *Polymer* **2013,** *54* (14), 3542-3547; (b)

Kwon, N. Y.; Kim, D.; Son, J. H.; Jang, G. S.; Lee, J. H.; Lee, T. S., Simultaneous Detection and Removal of Mercury Ions in Aqueous Solution with Fluorescent Conjugated Polymer-Based Sensor Ensemble. *Macromol Rapid Comm* **2011,** *32* (14), 1061-1065.

5. (a) Pu, K. Y.; Liu, B., Fluorescence Turn-on Responses of Anionic and Cationic Conjugated Polymers toward Proteins: Effect of Electrostatic and Hydrophobic Interactions. *J Phys Chem B* **2010,** *114* (9), 3077-3084; (b) Kwak, C. K.; Kim, D. G.; Kim, T. H.; Lee, C. S.; Lee, M.; Lee, T. S., Simultaneous and Dual Emissive Imaging by Micro-Contact Printing on the Surface of Electrostatically Assembled Water-Soluble Poly(p-phenylene) Using FRET. *Adv Funct Mater* **2010,** *20* (22), 3847-3855; (c) Yu, D. Y.; Zhang, Y.; Liu, B., Interpolyelectrolyte complexes of anionic water-soluble conjugated polymers and proteins as platforms for multicolor protein sensing and quantification. *Macromolecules* **2008,** *41* (11), 4003-4011; (d) Liu, B.; Bazan, G. C., Interpolyelectrolyte complexes of conjugated copolymers and DNA: Platforms for multicolor biosensors. *J Am Chem Soc* **2004,** *126* (7), 1942-1943.

6. Yang, N. J.; Liao, C. S.; Chen, S. A., Hysteresis in Conjugated Polymer Thin Film Transistors Generated by Chain Relaxation. *Adv Funct Mater* **2010,** *20* (6), 1000-1004.

7. Grimsdale, A. C.; Chan, K. L.; Martin, R. E.; Jokisz, P. G.; Holmes, A. B., Synthesis of Light-Emitting Conjugated Polymers for Applications in Electroluminescent Devices. *Chem Rev* **2009,** *109* (3), 897-1091.

8. (a) Duan, C. H.; Cai, W. Z.; Hsu, B. B. Y.; Zhong, C. M.; Zhang, K.; Liu, C. C.; Hu, Z. C.; Huang, F.; Bazan, G. C.; Heeger, A. J.; Cao, Y., Toward green solvent processable photovoltaic materials for polymer solar cells: the role of highly polar pendant groups in charge carrier transport and photovoltaic behavior. *Energ Environ Sci* **2013,** *6* (10), 3022-3034; (b) Yang, J. H.; Garcia, A.; Nguyen, T. Q., Organic solar cells from water-soluble poly(thiophene)/fullerene heterojunction. *Appl Phys Lett* **2007,** *90* (10); (c) Seo, J. H.; Gutacker, A.; Sun, Y. M.; Wu, H. B.; Huang, F.; Cao, Y.; Scherf, U.; Heeger, A. J.; Bazan, G. C., Improved High-Efficiency Organic Solar Cells via Incorporation of a Conjugated Polyelectrolyte Interlayer. *J Am Chem Soc* **2011,** *133* (22), 8416-8419; (d) Cheng, Y. J.; Yang, S. H.; Hsu, C. S., Synthesis of Conjugated Polymers for Organic Solar Cell Applications. *Chem Rev* **2009,** *109* (11), 5868-5923.

9. (a) Zhou, H. Q.; Zhang, Y.; Mai, C. K.; Collins, S. D.; Nguyen, T. Q.; Bazan, G. C.; Heeger, A. J., Conductive Conjugated Polyelectrolyte as Hole-Transporting Layer for Organic Bulk Heterojunction Solar Cells. *Adv Mater* **2014,** *26* (5), 780-785; (b) Zhang, L. J.; He, C.; Chen, J. W.; Yuan, P.; Huang, L. A.; Zhang, C.; Cai, W. Z.; Liu, Z. T.; Cao, Y., Bulk-Heterojunction Solar Cells with Benzotriazole-Based Copolymers as Electron Donors: Largely Improved Photovoltaic Parameters by Using PFN/A1 Bilayer Cathode. *Macromolecules* **2010,** *43* (23), 9771-9778; (c) He, Z. C.; Zhong, C. M.; Huang, X.; Wong, W. Y.; Wu, H. B.; Chen, L. W.; Su, S. J.; Cao, Y., Simultaneous Enhancement of Open-Circuit Voltage, Short-Circuit Current Density, and Fill Factor in Polymer Solar Cells. *Adv Mater* **2011,** *23* (40), 4636-+.

10. Pu, K. Y.; Li, K.; Liu, B., Multicolor Conjugate Polyelectrolyte/Peptide Complexes as Self-Assembled Nanoparticles for Receptor-Targeted Cellular Imaging. *Chem Mater* **2010,** *22* (24), 6736-6741.

11. Yang, R. Q.; Tian, R. Y.; Yan, J. G.; Zhang, Y.; Yang, J.; Hou, Q.; Yang, W.; Zhang, C.; Cao, Y., Deep-red electroluminescent polymers: Synthesis and characterization of new low-band-gap conjugated copolymers for light-emitting diodes and photovoltaic devices. *Macromolecules* **2005,** *38* (2), 244-253.

12. Liu, M. F.; Chen, Y. L.; Zhang, C.; Li, C. H.; Li, W. W.; Bo, Z. S., Synthesis of thiophene-containing conjugated polymers from 2,5-thiophenebis(boronic ester)s by Suzuki polycondensation. *Polym Chem-Uk* **2013,** *4* (4), 895-899.

13. Hou, J. H.; Chen, H. Y.; Zhang, S. Q.; Yang, Y., Synthesis and Photovoltaic Properties of Two Benzo[1,2-b:3,4-b ']dithiophene-Based Conjugated Polymers. *J Phys Chem C* **2009,** *113* (50), 21202-21207.

14. Yi, H. N.; Al-Faifi, S.; Iraqi, A.; Watters, D. C.; Kingsley, J.; Lidzey, D. G., Carbazole and thienyl benzo[1,2,5]thiadiazole based polymers with improved open circuit voltages and processability for application in solar cells. *J Mater Chem* **2011,** *21* (35), 13649-13656.

15. (a) Yao, K.; Chen, L.; Chen, Y. W.; Li, F.; Wang, P. S., Influence of water-soluble polythiophene as an interfacial layer on the P3HT/PCBM bulk heterojunction organic photovoltaics. *J Mater Chem* **2011,** *21* (36), 13780-13784; (b) da Silva, W. J.; Schneider, F. K.; Yusoff, A. B.; Jang, J., High performance polymer tandem solar cell. *Sci Rep-Uk* **2015,** *5*, 18090.
16. (a) Zhao, Z. Q.; Wu, Q. L.; Xia, F.; Chen, X.; Liu, Y. W.; Zhang, W. F.; Zhu, J.; Dai, S. Y.; Yang, S. F., Improving the Conductivity of PEDOT:PSS Hole Transport Layer in Polymer Solar Cells via Copper(II) Bromide Salt Doping. *ACS applied materials & interfaces* **2015,** *7* (3), 1439-1448; (b) Ratcliff, E. L.; Garcia, A.; Paniagua, S. A.; Cowan, S. R.; Giordano, A. J.; Ginley, D. S.; Marder, S. R.; Berry, J. J.; Olson, D. C., Investigating the Influence of Interfacial Contact Properties on Open Circuit Voltages in Organic Photovoltaic Performance: Work Function Versus Selectivity. *Adv Energy Mater* **2013,** *3* (5), 647-656; (c) Greiner, M. T.; Lu, Z. H., Thin-film metal oxides in organic semiconductor devices: their electronic structures, work functions and interfaces. *Npg Asia Mater* **2013,** *5*.
17. Bardeen, C., Exciton Quenching and Migration in Single Conjugated Polymers. *Science* **2011,** *331* (6017), 544-545.
18. (a) Mataga, N.; Tanimoto, O., Possible Mechanisms of Intermolecular Charge Transfer and Electron Transfer Processes in Excited Electronic State. *Theor Chim Acta* **1969,** *15* (2), 111-&; (b) Hutchison, G. R.; Ratner, M. A.; Marks, T. J., Intermolecular charge transfer between heterocyclic oligomers. Effects of heteroatom and molecular packing on hopping transport in organic semiconductors. *J Am Chem Soc* **2005,** *127* (48), 16866-16881.